JOURNAL OF BACTERIOLOGY, May 2008, p. 3283–3292 Vol. 190, No. 9
0021-9193/08/$08.00+0 doi:10.1128/JB.01934-07

DivIVA Is Required for Polar Growth in the MreB-Lacking Rod-Shaped Actinomycete *Corynebacterium glutamicum*▽†

Michal Letek,[1] Efrén Ordóñez,[1] José Vaquera,[2] William Margolin,[3] Klas Flärdh,[4] Luis M. Mateos,[1] and José A. Gil[1]*

Departamento de Biología Molecular, Área de Microbiología, Facultad de Biología, Universidad de León, León 24071, Spain[1]; Departamento de Biología Molecular, Área de Biología Celular, Facultad de Biología, Universidad de León, León 24071, Spain[2]; Department of Microbiology and Molecular Genetics, University of Texas Medical School, 6431 Fannin, Houston, Texas 77030[3]; and Department of Cell and Organism Biology, Lund University, 22362 Lund, Sweden[4]

Received 13 December 2007/Accepted 12 February 2008

The actinomycete *Corynebacterium glutamicum* grows as rod-shaped cells by zonal peptidoglycan synthesis at the cell poles. In this bacterium, experimental depletion of the polar DivIVA protein ($DivIVA_{Cg}$) resulted in the inhibition of polar growth; consequently, these cells exhibited a coccoid morphology. This result demonstrated that DivIVA is required for cell elongation and the acquisition of a rod shape. DivIVA from *Streptomyces* or *Mycobacterium* localized to the cell poles of $DivIVA_{Cg}$-depleted *C. glutamicum* and restored polar peptidoglycan synthesis, in contrast to DivIVA proteins from *Bacillus subtilis* or *Streptococcus pneumoniae*, which localized at the septum of *C. glutamicum*. This confirmed that DivIVAs from actinomycetes are involved in polarized cell growth. $DivIVA_{Cg}$ localized at the septum after cell wall synthesis had started and the nucleoids had already segregated, suggesting that in *C. glutamicum* DivIVA is not involved in cell division or chromosome segregation.

In rod-shaped bacteria such as *Escherichia coli* or *Bacillus subtilis*, cell division gives rise to hemispherical cell poles, which after their formation, largely remain inert (13). Bacterial cell elongation involves extension of the lateral cell wall, which in most rod-shaped bacteria occurs by intercalation of new peptidoglycan (PG) into the wall along most of its length. This process requires the assembly of MreB, an actin homologue, into a helical cytoskeleton that is distributed throughout the cell (7). In *E. coli*, the depletion of MreB results in the formation of coccoid cells (24). These observations suggest that the MreB-based cytoskeleton is involved in organizing or localizing enzymes that participate in cell wall assembly, such as penicillin-binding proteins, presumably through a linkage to the cell wall synthesis machinery via the proteins MreC, MreD, and RodA (6, 14, 24, 26).

A different and *mreB*-independent mode of cell elongation and rod shape acquisition is found among the corynebacteria. Similar to other members of the phylum *Actinobacteria* (gram-positive bacteria with a high G+C content in their DNA) that do not undergo sporulation (30), corynebacterial genomes are devoid of *mreB* homologues (8, 22, 30, 34, 43). Moreover, staining of the rod-shaped bacterium *Corynebacterium glutamicum* with fluorescently labeled vancomycin (vancomycin-Bodipy FL [Van-FL]) showed that PG is primarily assembled at the cell poles rather than along the lateral wall (11). In the simplest model describing the polarization of PG assembly in *C. glutamicum*, components of the cell division machinery are sufficient to recruit the enzymes for cell wall elongation to the new cell pole. However, the filamentous hyphal cells of another member of the *Actinobacteria*, *Streptomyces coelicolor*, grow by tip extension and incorporate new PG at the hyphal apex (18). This highly polarized mode of growth does not require cell division (31) and does not occur at the cell poles created by division. Instead, new hyphal tips are generated de novo either by branching or by the emergence of the germ tube, implying that the bacterium possesses a mechanism to establish apical cell wall assembly independent of the division process.

Observations in *C. glutamicum*, *S. coelicolor*, and, recently, in *Mycobacterium smegmatis* suggest that the coiled-coil protein DivIVA influences apical growth and cell shape determination (19, 33, 35). In these organisms, DivIVA has a distinct polar localization. The *divIVA* genes of *S. coelicolor* and *M. smegmatis* ($divIVA_{Sc}$ and $divIVA_{Ms}$, respectively) were found to be essential (19, 33), and this was also evidenced in *C. glutamicum* by the inability to obtain viable cells when the gene was deleted (19, 33, 35). Furthermore, in all three organisms, *divIVA* overexpression results in bloated asymmetric cells (19, 33, 35), whereas partial depletion of DivIVA in *S. coelicolor* affects tip extension and branching (19). In *Mycobacterium tuberculosis*, which also exhibits Van-FL staining patterns consistent with zonal PG biosynthesis at the poles (10), DivIVA is phosphorylated by the serine/threonine kinases PknA and PknB, and overexpression of *divIVA* or overexpression or partial depletion of these kinases was shown to alter the control of cell shape (23).

In this study, we addressed the basis for rod shape acquisition of *C. glutamicum*. The results showed that depletion of DivIVA leads to a coccoid morphology, and thus they provide evidence for the first time that DivIVA contributes to a mechanism by which cell growth and rod-shaped morphology are maintained via cell wall elongation at the poles. This function

* Corresponding author. Mailing address: Departamento de Biología Molecular, Área de Microbiología, Facultad de Biología, Universidad de León, 24071 León, Spain. Phone: 34 987 291503. Fax: 34 987 291479. E-mail: jagils@unileon.es.

† Supplemental material for this article may be found at http://jb.asm.org/.

▽ Published ahead of print on 22 February 2008.

could also be fulfilled by heterologous DivIVAs from other *Actinobacteria* but not by those from *B. subtilis* and *S. pneumoniae* from *Firmicutes*, suggesting that DivIVA functions differently in the two main phylogenetic lines of gram-positive bacteria.

MATERIALS AND METHODS

Bacterial strains and general methods for nucleic acids. Bacterial strains and plasmids are described in Table 1 (see Table S1 in the supplemental material for a description of the primers). *E. coli* cells were grown in Luria broth or Luria agar (20) complex medium at 37°C with aeration. *C. glutamicum* cells were grown in TSB (trypticase soy broth; Oxoid) or complex medium consisting of TSB containing 2% agar at 30°C. When required, the following supplements were added to the culture medium: kanamycin (50 μg/ml for *E. coli*; 12.5 μg/ml for corynebacteria), apramycin (50 μg/ml for *E. coli*; 12.5 μg/ml for corynebacteria), chloramphenicol (20 μg/ml for *E. coli*), ampicillin (100 μg/ml for *E. coli*), and tetracycline and streptomycin (12.5 μg/ml for *E. coli*).

Chromosomal DNA and plasmids were isolated, purified, digested, and labeled using conventional kits and protocols (28). Plasmids were transferred to the host by transformation (*E. coli*) or conjugation (*C. glutamicum*) following classical protocols (20, 29). Genetic constructions of *C. glutamicum* transconjugant strains were confirmed by Southern blot hybridization, using probes obtained by PCR amplification and labeled with digoxigenin according to the manufacturer's instructions (Boehringer Mannheim).

The correct design of plasmids expressing the different alleles used in this work required the characterization of the transcriptional control of *divIVA*. RNA was isolated from exponentially growing *C. glutamicum* in TSB medium using the RNeasy commercial kit (Qiagen). Rapid amplification of cDNA ends (RACE)-PCR experiments were carried out according to the protocol provided with a 5′/3′ RACE Kit, 2nd Generation (Roche). To identify promoters located upstream from *divIVA*, 2 μg of total RNA was used as a template to generate single-strand cDNA using primer race1 (see Table S1 in the supplemental material). A homopolymeric A tail was added to the 3′ end of the purified cDNA preparation using terminal transferase, and the dA-tailed cDNA was used in two further PCR amplification steps. In the first one, the primers dT/race2 (see Table S1 in the supplemental material) were used; the amplified DNA product of this reaction then served as the substrate in the second PCR amplification, using the primers dT/race3 (see Table S1 in the supplemental material). The amplified fragments were cloned into pGEM-TEasy vector (Table 1) based on a T-A cloning technique and used to transform *E. coli* TOP10. Ten plasmids isolated from different clones were sequenced; all of them started with the same G residue, located 80 nucleotides upstream from the ATG start codon of *C. glutamicum divIVA* (*divIVA*$_{Cg}$).

Computer analyses were carried out with DNASTAR (DNAstar, Inc., London, United Kingdom), database similarity searches were done at the BLAST and FASTA public servers (NCBI, Bethesda, MD), and multiple alignments of sequences were carried out using Clustal W (EBI, Hinxton Hall, United Kingdom). Plasmid constructions (Table 1) were confirmed to be correct by sequencing using the dideoxy nucleotide chain termination method of Sanger (37).

Construction of recombinant plasmids. The *divIVA*$_{Cg}$ gene was PCR amplified using the primers div1/2 (see Table S1 in the supplemental material). The adequate PCR product was cloned into plasmid pET28a by NdeI-EcoRI digestion, giving rise to the vector pETDIV (Table 1). pETDIV allowed the expression and purification of the *C. glutamicum* DivIVA (DivIVA$_{Cg}$) protein with an N-terminal His tag, which was used for the production of polyclonal anti-DivIVA$_{Cg}$ antibodies (see below).

Plasmids pOJD and pOJPD were designed to disrupt the chromosomal copy of *divIVA*$_{Cg}$ and to place a second copy of *divIVA*$_{Cg}$ under the control of the regulated promoters P*lac* or P*gntP*. To construct pOJD, a 498-bp 5′ region of *divIVA*$_{Cg}$ was obtained by NdeI-NaeI digestion of the plasmid pETDIV. This DNA fragment was blunted by Klenow treatment and then ligated into the EcoRV-digested pOJ260 plasmid, yielding the vector pOJD (Table 1). To construct pOJPD, a 770-bp DNA fragment was obtained by EcoRV-NaeI digestion of plasmid pEPDG (Table 1). The product of this digestion carried the P*gntP* promoter fused to the 498-bp *divIVA*$_{Cg}$ 5′ region. This DNA fragment was subcloned into EcoRV-digested pOJ260, yielding the plasmid pOJPD (Table 1).

To easily clone any promoterless gene under the control of the P*div*$_{Cg}$ promoter and fuse it to the *egfp2* gene (encoding an enhanced green fluorescent protein) at the same time, a new NdeI site overlapping the start codon of *divIVA*$_{Cg}$ was generated in plasmid pEAG2 (35). This was done by PCR mutagenesis using the specific primers listed in Table S1 in the supplemental material, yielding the plasmid pEAG3. The *divIVA* genes, without their stop codons, from *B. subtilis*, *S. coelicolor*, *S. pneumoniae*, and *M. tuberculosis* were then PCR amplified from their corresponding chromosomal DNAs using the primers listed in Table S1 in the supplemental material. The PCR products were cloned into the NdeI-digested pEAG3 plasmid, yielding the bifunctional mobilizable vectors pEBSE (for *B. subtilis divIVA* [*divIVA*$_{Bs}$]), pESCE (for *S. coelicolor divIVA*$_{Sc}$), pESPE (for *S. pneumoniae divIVA* [*divIVA*$_{Sp}$]), and pEMTE (for *M. tuberculosis divIVA* [*divIVA*$_{Mt}$]) (Table 1).

To overexpress the above-mentioned *divIVA* genes (hereafter *divIVA*$_{NN}$) without fusion to *egfp2*, these genes, including their stop codons and the promoter P*div* sequence, were PCR amplified from plasmids pEBSE, pESCE, pESPE, and pEMTE using the primers listed in Table S1 in the supplemental material. The corresponding PCR products were then subcloned by EcoRV digestion into the pECM2 plasmid (Table 1), yielding the vectors pEBS, pESC, pESP, and pEMT.

To introduce a copy of the DNA fragments comprising P*div-divIVA*$_{NN}$*-egfp2* into the *C. glutamicum* chromosome, the plasmids pEAG3 and pEBSE, pESCE, pESPE, and pEMTE were digested with EcoRV-SmaI; the obtained DNA fragments were then subcloned into the EcoRV-digested pK18-3 plasmid, giving rise to the vectors pK18-CGE, -BSE, -SCE, -SPE, and -MTE (Table 1). Similarly, plasmids pEBS, pESC, pESP, and pEMT were digested with EcoRV, and the fragments containing only the P*div-divIVA*$_{NN}$ genes, i.e., not fused to the *egfp2* gene, were subcloned into EcoRV-digested pK18-3 plasmid, yielding the vectors pK18-BS, -SC, -SP, and -MT (Table 1). In contrast, plasmid pK18-CG was constructed by direct cloning of a PCR-amplified fragment containing P*div-divIVA*$_{Cg}$ into the EcoRV-digested vector pK18-3 (Table 1).

As a negative control for the gene complementation experiments, the plasmid pK18-E was constructed. To do so, plasmid pEAG3 was digested with NdeI and religated, giving rise to pEAGE (P*div-egfp2*) (Table 1). A fragment containing P*div-egfp2* was obtained by EcoRV-SmaI digestion of pEAGE and then subcloned into the EcoRV-digested pK18-3 plasmid, yielding the vector pK18-E (Table 1).

Two-hybrid system assays. To construct the plasmids for the two-hybrid assays, the *divIVA* genes from *C. glutamicum*, *B. subtilis*, *S. coelicolor*, *S. pneumoniae*, and *M. tuberculosis* were PCR amplified by using specific primers (see Table S1 in the supplemental material) and cloned separately into pBT (bait) and pTRG (target/prey) vectors (BacterioMatch II Two-Hybrid System Vector Kit; Stratagene) (Table 1), yielding a series of pBTD and pTRGD plasmids carrying the respective *divIVA* genes (Table 1). Bait and prey plasmids were cotransformed into the *E. coli* BacterioMatch II reporter strain (Table 1) and analyzed as previously described (44).

Protein isolation and manipulation. *C. glutamicum* cells were disrupted using FastPROTEIN Blue Lysing Matrix (Qbiogene Inc., Carlsbad, CA) and the BIO101 Thermo Savant FastPrep FP120 (Qbiogene Inc.) as described previously (27). The amount of protein present in cell extracts was quantified by a Bradford assay (5). Proteins were separated by sodium dodecyl sulfate-polyacrylamide gel electrophoresis (25), stained with Coomassie blue or electroblotted onto polyvinylidene difluoride membranes (Millipore), and immunostained with a 1:10,000 dilution of rabbit polyclonal antibodies raised against green fluorescent protein (GFP) or His tags (Santa Cruz Biotechnology) and with guinea pig polyclonal antibodies raised against purified His-tagged DivIVA$_{Cg}$ (see below). Anti-rabbit or anti-guinea pig immunoglobulin G-alkaline phosphatase (Santa Cruz Biotechnology) was used as the secondary antibody at a 1:10,000 dilution.

To monitor the cellular content of DivIVA$_{Cg}$ and localize the protein by immunofluorescence microscopy, antiserum was raised against the *divIVA*$_{Cg}$ gene product as follows: *E. coli* BL21(DE3) cells (Table 1) were transformed with plasmid pETDIV (Table 1) and induced with isopropyl-β-D-thiogalactopyranoside, and the His-tagged DivIVA$_{Cg}$ protein was purified by one-step Ni^{2+} affinity chromatography (His-Bind; Novagen). This His-tagged protein was used to immunize male guinea pigs (66-day immunization protocol) for the production of polyclonal anti-DivIVA$_{Cg}$ antibodies. The resulting polyclonal antibodies specifically recognized a protein of ~38 kDa, the expected size of DivIVA$_{Cg}$.

Microscopy. *C. glutamicum* cells containing the constructs carrying GFP or stained with fluorescent dyes (see later) were observed with a Nikon E400 fluorescence microscope. Photographs were taken with a DN100 Nikon digital camera and assembled using Corel Draw.

Van-FL (green fluorescence) or vancomycin-Bodipy 650/665 ([Van-650/665] red fluorescence; Molecular Probes) staining was done by adding equal proportions of unlabeled vancomycin and Van-FL or Van-650/665 to growing cultures at a final concentration of 1 μg/ml (11). The culture was then incubated for 5 min to allow adsorption of the antibiotic, after which the cells were viewed directly by fluorescence microscopy.

DAPI (4′,6-diamino-2-phenylindole) staining and immunofluorescence microscopy were carried out as described previously (12), except that *C. glutamicum*

TABLE 1. Bacterial strains and plasmids

Strain or plasmid	Relevant genotype or description[a]	Source and/or reference
E. coli strains		
TOP10	F$^-$ *mcr*A Δ(*mrr-hsdRMS-mcrBC*) φ80*lacZ*Δ*M15* Δ*lacX74 deoR recA1 araD139* Δ(*ara-leu*)*7697 galU galK rpsL endA1 nupG*; used for general cloning	Invitrogen
BL21(DE3)	F$^-$ *ompT hsdS*$_B$(r_B^- m_B^-) *gal dcm* (DE3); used for in vivo gene expression	Novagen
S17-1	*pro recA*; mobilizing donor strain that has an RP4 derivative integrated into the chromosome	39
XL1-Blue MRF′	Host strain used for propagating pBT and pTRG recombinants	Stratagene
BacterioMatch II	Reporter strain derived from Stratagene's XL1-Blue MR, harbors *lacI*^{q} and the reporter genes *HIS3* and *aadA* on the F′ episome	Stratagene
C. glutamicum strains		
ATCC 13869	Wild type	ATCC
R31	ATCC 13869 derivative; used as recipient in conjugation assays and as control strain	38
LACD	R31 derivative obtained by integration of plasmid pOJD; Apr^r	This work
LACID	LACD derivative containing the bifunctional plasmid pALacI; Apr^r Kan^r	This work; Fig. 1B
R33	R31 derivative containing *divIVA*$_{Cg}$*-egfp2* under the control of P*div* (P*div-divIVA*$_{Cg}$*-egfp2*) by integration of plasmid pK18-CGE; Kan^r	This work; Fig. 5B
GNTD	R31 derivative containing a complete copy of *divIVA*$_{Cg}$ under the control of P*gntP* by integration of plasmid pOJPD; Apr^r	This work
GNTCG, GNTBS, GNTSC, GNTSP, GNTMT	GNTD derivatives containing the respective *divIVA* genes under the control of *Pdiv* (P*div-divIVA*) by integration of plasmids pK18-CG, -BS, -SC, -SP, and -MT respectively; Apr^r Kan^r	This work; Fig. 2A
GNTD3	GNTD derivative containing the plasmid pK18–3 integrated in the chromosome; Apr^r Kan^r	This work; Fig. 2A
GNTCGE, GNTBSE, GNTSCE, GNTSPE, GNTMTE	GNTD derivatives containing the respective *divIV-egfp2* genes under the control of the P*div* promoter (P*div-divIVA_egfp2*) by integration of plasmids pK18-CGE, -BSE, -SCE, -SPE, -MTE, respectively; Apr^r Kan^r	This work; Fig. 2B
GNTDE	GNTD derivative containing *egfp2* under the control of P*div* promoter (P*div-egfp2*) by integration of plasmid pK18-E; Apr^r Kan^r	This work; Fig. 2B
AG1	R31 derivative containing the bifunctional mobilizable plasmid pEAG1; Kan^r Cat^r	This work; Fig. 3
AG3	R31 derivative containing the bifunctional mobilizable plasmid pEAG3; Kan^r Cat^r	This work; Fig. 3
BS, SC, SP, MT	R31 derivatives containing the bifunctional mobilizable plasmids pEBS, pESC, pESP, and pEMT respectively; Kan^r Cat^r	This work; Fig. 3
BSE, SCE, SPE, MTE	R31 derivatives containing the bifunctional mobilizable plasmids pEBSE, pESCE, pESPE, and pEMTE respectively; Kan^r Cat^r	This work; Fig. 3
Plasmids		
pET28a	*E. coli* expression vector; *kan*	Novagen
pETDIV	pET28a derivative carrying the His$_6$-tagged *divIVA*$_{Cg}$ gene	This work
pGEM-TEasy	*E. coli* vector; *bla lacI orif1*	Promega
pECM2	Mobilizable plasmid capable of replicating in *E. coli* and *C. glutamicum*; *kan cat*	21
pEAG1	pECM2 derivative carrying P*div-divIVA*$_{Cg}$	35
pEAG2	pEAG1 derivative carrying P*div-divIVA*$_{Cg}$*-egfp2*	35
pEAG3	pEAG2 derivative including an extra NdeI site between *divIVA*$_{Cg}$*-egfp2* and P*div*	This work
pEAGE	pEAG3 derivative carrying *Pdiv-egfp2* and used to construct pK18-3	This work
pEGFP	pECM2 derivative carrying *egfp2* under the control of the P*kan* and flanked by transcriptional terminators T1 and T2	28
pEGNC	pEGFP derivative carrying the promoterless *egfp2* gene	28
pEPDG	pEGFP derivative carrying P*gntP-divIVA*$_{Cg}$*-egfp2*	28
pOJ260	Mobilizable plasmid carrying an *E. coli* origin of replication and the *apr* resistance determinant	4
pOJD	pOJ260 derivative carrying the 5′ end of *C. glutamicum divIVA*$_{Cg}$ under the control of the promoter P*lac* (P*lac-*Δ*divIVA*$_{Cg}$)	This work
pOJPD	pOJ260 derivative carrying the 5′ end of *C. glutamicum divIVA*$_{Cg}$ under the control of the promoter of the *C. glutamicum gntP* gene (P*gntP-*Δ*divIVA*$_{Cg}$)	This work
pAlacI	Mobilizable plasmid capable of replicating in *E. coli* and *C. glutamicum*; *lacI*^{q} *kan*	45
pK18-3	Mobilizable plasmid carrying an *E. coli* origin of replication, *kan* and three *C. glutamicum* ORFs of unknown function located downstream from *ftsZ*	1
pEBSE, pESCE, pESPE, pEMTE	pEAG3 derivatives carrying the respective P*div-divIVA-egfp2* gene fusion	This work
pEBS, pESC, pESP, pEMT	pECM2 derivatives carrying the respective P*div-divIVA* gene fusion	This work
pK18-CGE, -BSE, -SCE, -SPE, -MTE	pK18-3 derivatives carrying the respective P*div-divIVA-egfp2* gene fusion	This work
pK18-E	pK18-3 derivative carrying P*div-egfp2*	This work
pK18-CG, -BS, -SC, -SP, -MT	pK18-3 derivatives carrying the respective P*div-divIVA* gene fusion	This work
pBT	Two-hybrid system bait plasmid containing the *cat* gene, p15A origin of replication and λ cI ORF	Stratagene
pBTD$_{Cg}$, pBTD$_{Bs}$, pBTD$_{Sc}$, pBTD$_{Sp}$, pBTD$_{Mt}$	pBT derivatives carrying the respective *divIVA* genes	This work
pTRG	Two-hybrid system target plasmid containing the *tet* gene, ColE1 origin of replication, and RNA polymerase α subunit ORF	Stratagene
pTRGD$_{Cg}$, pTRGD$_{Bs}$, pTRGD$_{Sc}$, pTRGD$_{Sp}$, pTRGD$_{Mt}$	pTRG derivatives carrying the respective *divIVA* genes	This work

[a] Apr^r, Kan^r, and Cat^r indicate resistance to apramycin, kanamycin, and chloramphenicol, respectively; *bla, kan, apr*, *cat*, and *tet* are the ampicillin, kanamycin, apramycin, chloramphenicol, and tetracycline resistance genes, respectively. ORF, open reading frame.

cells were permeabilized for 4 h at 30°C with lysozyme (10 μg/ml). The permeabilized cells were then incubated with a 1:1,000 dilution of anti-DivIVA$_{Cg}$ antiserum for 1 h and then for another hour with a 1:10,000 dilution of anti-guinea pig fluorescein-conjugated secondary antibody (Santa Cruz Biotechnology).

For transmission electron microscopy, cell pellets were rinsed three times in water, resuspended in 2.5% glutaraldehyde in phosphate buffer (pH 7), and fixed for 1 h. The cells were then rinsed three times in phosphate buffer and centrifuged at 1,600 × *g*; the cell pellet was mixed with 1% agarose and processed as described previously (46). The samples were infiltrated with epon-araldite,

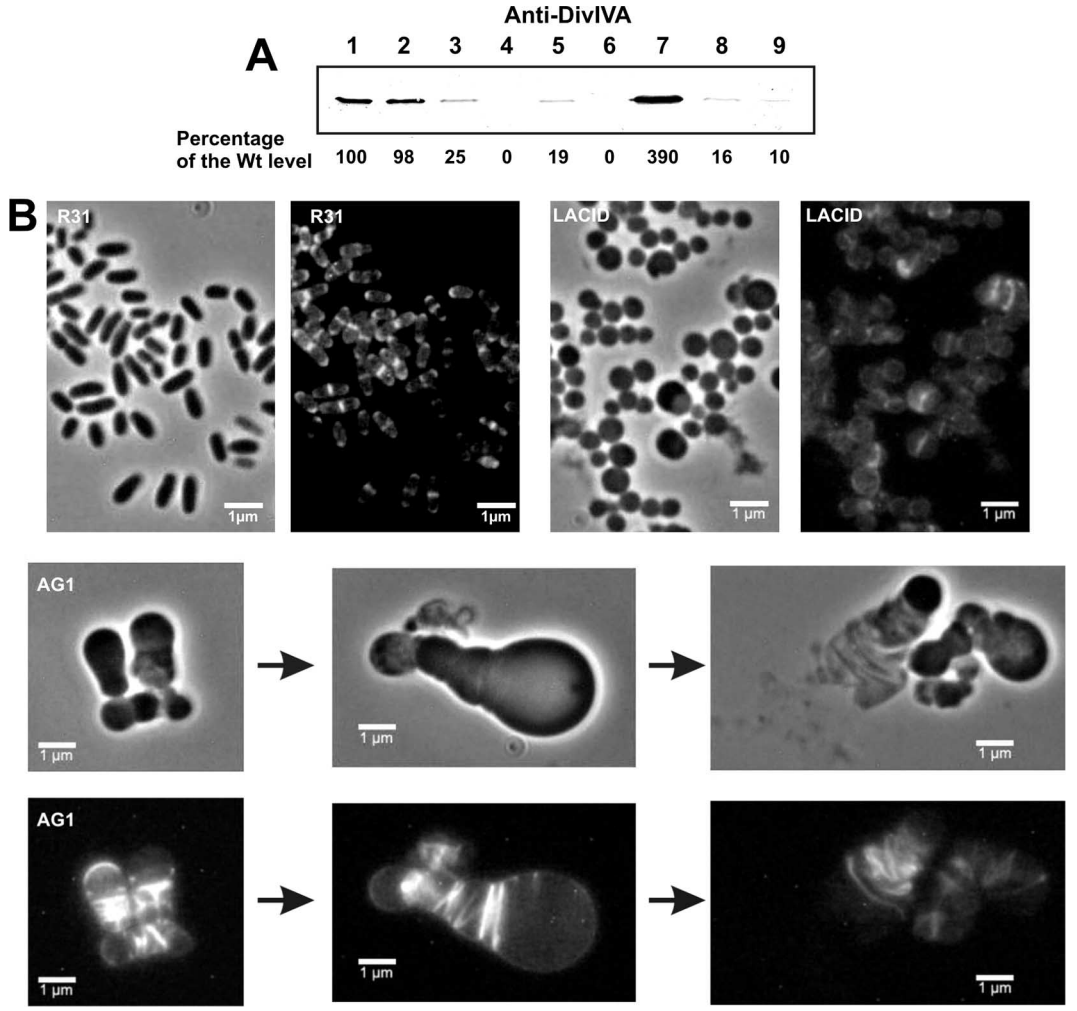

FIG. 1. Effect of DivIVA depletion on cell shape and polar growth of *Corynebacterium glutamicum*. (A) Quantitative Western blot of DivIVA from different exponentially grown *C. glutamicum* strains. Lane 1, strain R31; lane 2, strain R31 plus 4%Suc; lane 3, strain GNTD (P*gntP-divIVA*$_{Cg}$); lanes 4 and 8, strain GNTD grown in 4%Suc; lane 5, strain LACD (P*lac-divIVA*$_{Cg}$); lanes 6 and 9, strain LACID (P*lac-divIVA*$_{Cg}$ *lacI*^{q}); lane 7, strain AG1 (multicopy *divIVA*$_{Cg}$). Ten micrograms of cell extract proteins was used in lanes 8 and 9; otherwise, 1 μg was loaded per lane. (B) Phase-contrast and Van-FL staining of exponentially growing cells. The typical morphology of *C. glutamicum* R31 was converted to a coccoid morphology (no polar growth) in strain LACID, which is depleted of DivIVA. In *C. glutamicum* LACID the zonal PG synthesis is absent whereas strain AG1 (multicopy *divIVA*$_{Cg}$) grows apically and forms many apparently incomplete septa. Wt, wild type.

blocked, and polymerized at 55°C (blocks). From the blocks, ultrathin sections (70 nm thick) were obtained using a Leica Ultracut UCT ultramicrotome and placed on 200-mesh bare copper grids. Sections were stained with 0.5% aqueous lead citrate and then with 4% aqueous uranyl acetate and examined in a LEO EM910 transmission electron microscope operated at 80 kV. Images were taken at various magnifications using a Gatan 792 BioScan digital camera (1024 by 1024 pixels).

RESULTS

Partial depletion of DivIVA causes loss of the rod shape. In *C. glutamicum*, *divIVA* seems to be an essential gene, as in a previous study no null mutants were obtained (35). We therefore investigated the function of the *divIVA* gene product by conditional gene expression using two promoters able to regulate the expression of essential genes in *C. glutamicum*: P*lac* (36) and P*gntP* (28). Accordingly, *C. glutamicum* was transformed with the suicide plasmids pOJD (P*lac*-Δ*divIVA*$_{Cg}$) or pOJPD (P*gntP*-Δ*divIVA*$_{Cg}$) (Table 1). These plasmids are unable to replicate autonomously in *C. glutamicum* and carry truncated copies of *divIVA*$_{Cg}$ under the control of regulated promoters. When introduced into *C. glutamicum*, the plasmids integrate by homologous recombination into the chromosomal *divIVA* locus, leaving a disrupted copy of the gene under its natural promoter and a full-length version under the control of the promoter P*lac* or P*gntP*. Southern blot analysis of DNAs obtained from the transconjugant strains *C. glutamicum* LACD and GNTD (Table 1) showed the pattern expected for Campbell-type integration of plasmids pOJD and pOJPD, respectively, at the chromosomal *divIVA* locus (see Fig. S1 in the supplemental material).

Quantitative Western blot analysis of strains LACD and GNTD revealed that the level of DivIVA was reduced to 19 and 25% of wild-type levels, respectively (Fig. 1A). DivIVA depletion was more evident when the *E. coli lacI*^{q} gene present on plasmid pALacI (Table 1) was transferred to strain LACD

to repress the *lac* promoter (yielding strain LACID) (Table 1) or when strain GNTD was grown in the presence of 4% sucrose (4%Suc), which was previously shown to strongly repress P*gntP* (28). For strains LACID and GNTD (the latter grown on 4%Suc), DivIVA levels were estimated to be 1.0 and 1.6%, respectively, of those normally present in the wild-type strain (Fig. 1A, lanes 4, 6, 8, and 9).

The only band detected in Western blot analyses using anti-DivIVA antibodies was the corresponding 38-kDa full-length protein. Therefore, it can be assumed that the genetic methods used to disrupt the chromosomal copy of $divIVA_{Cg}$ did not result in partial DivIVA proteins that may have interfered with the analysis. A polar effect was not expected because of the monocistronic character of the transcript (35). These data confirmed that the observed effects described below were due only to the partial depletion of DivIVA.

The *C. glutamicum* LACD strain, expressing *divIVA* from P*lac*, had a coccoid phenotype and thus was morphologically clearly different from the rod-shaped cells of the parent strain *C. glutamicum* R31. A similar phenotype was obtained when the level of DivIVA was lowered even further in the LACID strain (Fig. 1B), although the strain's growth rate was lower than that of strain LACD (see Fig. S2A in the supplemental material). The same coccoid phenotype was obtained when strain GNTD was grown in TSB alone or in TSB plus 4%Suc to repress the expression of P*gntP* (data not shown). The coccoid shape assumed by the cells after DivIVA depletion suggested that cell elongation was perturbed. To test this idea, cells from strains R31 and LACID were stained with Van-FL. As reported previously (11), Van-FL staining confirmed the incorporation of new PG at the cell poles and septum of *C. glutamicum* R31 (Fig. 1B). In sharp contrast, in strain LACID, which has only 1% of the normal level of DivIVA and exhibits a coccoid phenotype, PG synthesis was detected mainly as bands in the middle of the cells (Fig. 1B). When $divIVA_{Cg}$ was introduced in *trans* through the integrating plasmid pK18-CG (Table 1) into the DivIVA-depleted strain GNTD, normal *divIVA* expression and cell shape were restored (see below).

Function of heterologous DivIVA proteins in *C. glutamicum*. We analyzed whether DivIVA proteins from other species could restore polarized growth and a rod shape to *C. glutamicum* GNTD (Table 1), in which $DivIVA_{Cg}$ is depleted. These experiments could not be carried out on strain LACID due to the resistance markers present on pALacI and the plasmids used to deliver heterologous *divIVA* genes. The *divIVA* genes from two representatives of each of the two main phylogenetic lineages of gram-positive bacteria were tested (Fig. 2): $divIVA_{Sc}$ and $divIVA_{Mt}$ from *Actinobacteria* and $divIVA_{Bs}$ and $divIVA_{Sp}$ from the *Firmicutes*. The exogenous genes were cloned behind the $divIVA_{Cg}$ promoter (P*div*), and the construct was inserted as a single copy by homologous recombination into the region upstream from *divIVA* in the *C. glutamicum* GNTD chromosome (Fig. 2A), as previously described for other genes (1). Similar constructs carrying translational fusions between *divIVA* genes and *egfp2* were also produced and integrated into strain GNTD (Fig. 2B). Southern blotting and PCR analysis of the transconjugants indicated that integration of the suicide plasmids took place at the expected site (see Fig. S3 in the supplemental material).

Strain *C. glutamicum* GNTD had a coccoid morphology that reverted to the typical corynebacterial shape when the gene $divIVA_{Cg}$, $divIVA_{Sc}$, or $divIVA_{Mt}$ was inserted into the chromosome, resulting in strains GNTCG, GNTSC, and GNTMT, respectively (Fig. 2A; Table 1). Similar results were obtained with $divIVA_{Cg}$, $divIVA_{Sc}$, and $divIVA_{Mt}$ fused to *egfp2* in strains GNTCGE, GNTSCE, and GNTMTE, respectively (Fig. 2B). As negative controls, *C. glutamicum* GNTD was transformed with the empty vector pK18-3 or pK18-E (the latter carrying the promoter-less *egfp2* gene under P*div*) (Table 1), leading to strains GNTD3 and GNTDE, respectively (Table 1), in which the coccoid phenotype was maintained (Fig. 2A and B). Van-FL staining of polar cell wall synthesis, which was not detected in the depletion strains *C. glutamicum* GNTD (not shown) or GNTD3, became visible again after integration of $divIVA_{Cg}$, $divIVA_{Sc}$, or $divIVA_{Mt}$ (Fig. 2A). Furthermore, distinctive localization of the EGFP2-tagged gene products of either $divIVA_{Sc}$ or $divIVA_{Mt}$ to the cell poles and septation sites was similar to that of $DivIVA_{Cg}$-EGFP2 (Fig. 2B).

In contrast, when $divIVA_{Bs}$ and $divIVA_{Sp}$ were introduced in the same way into strain GNTD to generate GNTBS and GNTSP, respectively (Table 1), polar Van-FL staining was not observed in either case (Fig. 2A). Moreover, the presence of these genes appeared to be toxic, such that the growth rates of these strains were reduced compared to growth of the parent strain GNTD (see Fig. S2B in the supplemental material). Although cells from GNTBS and GNTSP were elongated, this did not seem to be a result of polar growth but rather of aberrant septation and failure of the daughter cells to separate. None of the EGFP2-fused DivIVA proteins from *B. subtilis* or *S. pneumoniae* showed a polar localization in *C. glutamicum*. In the case of strain GNTBSE ($divIVA_{Bs}$-*egfp2*), the fusion protein was mainly targeted to cell division sites, leading to modestly filamentous cells and the appearance of several septa (Fig. 2B). Strain GNTSPE ($divIVA_{Sp}$-*egfp2*) showed very little fluorescence, but the morphology of this strain and the shape of the cells, together with Van-FL staining of GNTSP (Fig. 2A), suggested that $divIVA_{Sp}$ expression inhibits a late stage of cell division or cell separation in *C. glutamicum*. All EGFP2-fused proteins were detected in cell extracts using anti-GFP antibodies (see Fig. S3B in the supplemental material). The only exception was $DivIVA_{Sp}$-EGFP2, which appeared to be unstable, and there was no detectable fluorescence in the transconjugant strain GNTSPE.

Homologous overexpression of $divIVA_{Cg}$ was previously shown to cause pronounced effects on cell morphology, with large and asymmetric swollen cells in which DivIVA-EGFP2 accumulated, often asymmetrically, at the cell poles (35). This provided a second approach to test the activities of heterologous *divIVA* genes in *C. glutamicum*, i.e., whether their expression had the same effect on cell morphology as overexpression of the native gene. PCR-amplified heterologous *divIVA* genes were placed under the control of the $divIVA_{Cg}$ promoter (P*div*) by exchanging them with $divIVA_{Cg}$ in the multicopy plasmid pEAG3 (Table 1) and fused at their 3′ end to *egfp2* (P*div*-$divIVA_{Cg}$-*egfp2*). These genes were also subcloned with P*div* but without *egfp2* (P*div*-$divIVA_{Cg}$) in the same vector, which has a copy number of 30 to 40 per cell (36). The resulting sets of plasmids (the set pEBSE, pESCE, pESPE, and pEMTE and the set pEBS, pESC, pESP, and pEMT, with and without fusion to *egfp2*, respectively) (Table 1) allowed multicopy ex-

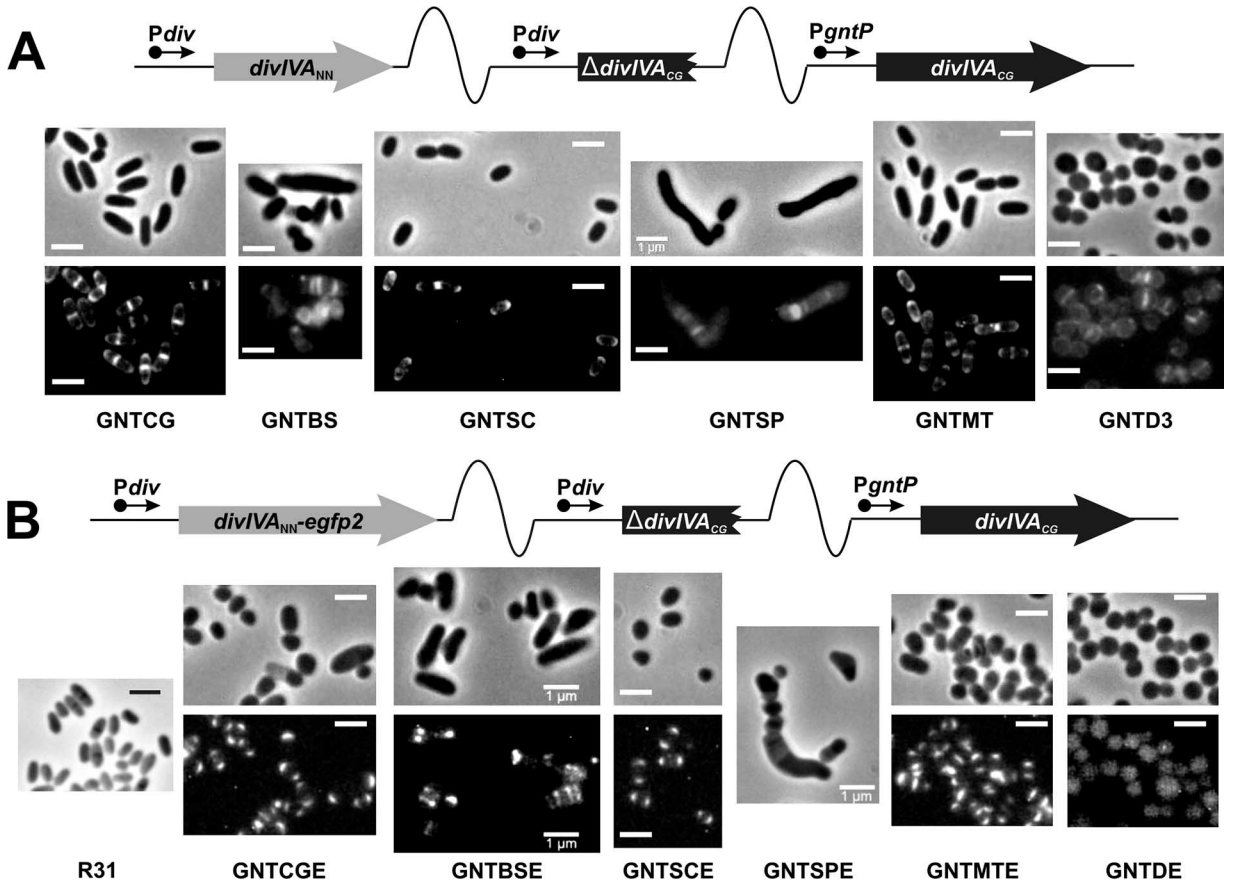

FIG. 2. Actinomycete DivIVAs restore polar growth and a rod shape to DivIVA$_{Cg}$-depleted *C. glutamicum* cells. (A) Schematic representation of the integration of plasmids pK18-CG, -BS, -SC, -SP, and -MT carrying P*div-divIVA* from *C. glutamicum* (strain GNTCG), *B. subtilis* (strain GNTBS), *S. coelicolor* (strain GNTSC), *S. pneumoniae* (strain GNTSP), or *M. tuberculosis* (strain GNTMT) as a single copy into the chromosome of *C. glutamicum* GNTD. Integration of the empty vector pK18-3 in the chromosome of *C. glutamicum* GNTD was used as a negative control (strain GNTD3). All strains were grown in 4%Suc, and fluorescence images of Van-FL staining (lower panels) and phase-contrast images of the cells (upper panels) are shown. Reversion of the coccoid morphology to yield rod-shaped cells and polar/septal rather than septal Van-FL staining was observed with *Actinobacteria* DivIVAs but not with *Firmicutes* DivIVAs. Size bar, 1 μm. (B) Schematic representation of the integration of plasmids pK18-CGE, -BSE, -SCE, -SPE, and -MTE carrying P*div-divIVA-egfp2* from *C. glutamicum* (strain GNTCGE), *B. subtilis* (strain GNTBSE), *S. coelicolor* (strain GNTSCE), *S. pneumoniae* (strain GNTSPE), or *M. tuberculosis* (strain GNTMTE) as a single copy into the chromosome of *C. glutamicum* GNTD. Integration of the plasmid pK18-E in the chromosome of *C. glutamicum* GNTD was used as a negative control (strain GNTDE). All strains were grown in 4%Suc, and fluorescence images of EGFP2 (lower panels) and phase-contrast images of the cells (upper panels) are shown. Reversion of the coccoid morphology to yield rod-shaped cells and polar localization of the fused proteins was observed with *Actinobacteria* DivIVAs but not with *Firmicutes* DivIVAs. The morphology of the parent strain R31 is provided for comparison. Size bar, 1 μm.

pression of the different *divIVA* genes. The results showed that the effects on morphology were similar with or without fusion to *egfp2*. Overexpression of *divIVA*$_{Cg}$ led to large and bulky cells, often with shapes reminiscent of "ice cream cones" (Fig. 1B and 3, strains AG1 and AG3). In these cells, active assembly of PG was detected mainly at one pole and/or in multiple apparent cross-walls inside the cell (Fig. 1B). In the case of *divIVA*$_{Mt}$ and *divIVA*$_{Sc}$ (strains GNTMT and GNTSC, respectively) (Table 1), the morphologies of the cells were similar to that resulting from *divIVA*$_{Cg}$ overexpression, and the EGFP2 fusion proteins (strains GNTMTE and GNTSCE) accumulated as a large cluster at one cell pole (Fig. 3A). Overexpression of *divIVA*$_{Bs}$ or *divIVA*$_{Sp}$ also led to aberrant morphologies (strains GNTBS and GNTSP) but, in contrast to the other proteins, DivIVA$_{Bs}$ or DivIVA$_{Sp}$ fused to EGFP2 localized at mid-cell or in multiple septa and never clearly accumulated at the cell poles (Fig. 3A, *C. glutamicum* BSE and *C. glutamicum* SPE).

Transmission electron microscopy images indicated that overexpression of the *divIVA* genes perturbed cell division (Fig. 3B); multiple septa were visible, but they were incomplete and were not associated with cell separation. These results were confirmed by Van-FL staining (data not shown). A negative effect on cell growth was also observed (Fig. S2C, GNTBS and GNTSP). Antibodies against GFP were used to measure protein levels in the strains carrying the DivIVA$_{NN}$-EGFP2 fusion. The levels were similar in all cases, except for the DivIVA$_{Sp}$-EGFP2 hybrid, which was most likely less stable than the other fusion proteins (see above).

Interactions between heterologous DivIVA proteins. DivIVA$_{Bs}$ has been reported to interact with itself, presumably through coiled-coil regions, to form an oligomeric structure (32, 33, 42).

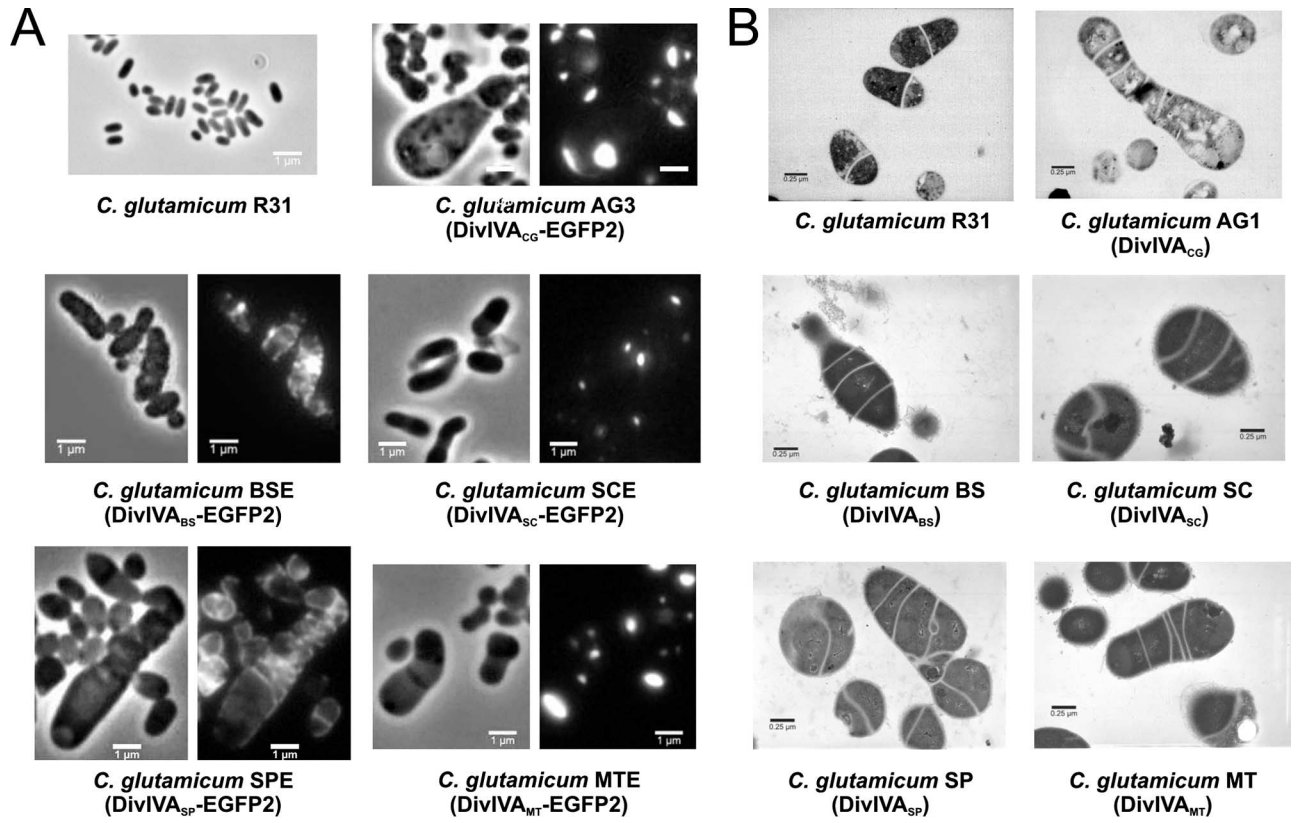

FIG. 3. Effect on *C. glutamicum* of the overproduction of DivIVA proteins from different gram-positive bacteria. (A) Fluorescence images of EGFP2 (right panels) and phase-contrast images (left panels) of the different *C. glutamicum* strains overexpressing *divIVA* fused to *egfp2* from *C. glutamicum* (strain AG3), *B. subtilis* (strain BSE), *S. coelicolor* (strain SCE), *S. pneumoniae* (strain SPE), or *M. tuberculosis* (strain MTE). Note that polar and septal localization of DivIVA was achieved only with DivIVA-EGFP2 from actinomycetes. (B) Transmission electron micrographs of exponentially growing cells of different *C. glutamicum* strains overexpressing *divIVA* from *C. glutamicum* (strain AG1), *B. subtilis* (strain BS), *S. coelicolor* (strain SC), *S. pneumoniae* (strain SP), or *M. tuberculosis* (strain MT). *C. glutamicum* R31 was included as a control.

We therefore measured the capacity for self-interaction of DivIVA using a bacterial two-hybrid system. All five tested DivIVAs self-interacted when present on both bait and prey plasmids (pBT, pTRG, and its corresponding plasmids series) (Table 1) and allowed *E. coli* reporter cells to grow in minimal selective medium. The results (Fig. 4) are consistent with the idea that DivIVA proteins exist as oligomers in their hosts. DivIVA$_{Cg}$ was found to interact only with actinomycete DivIVAs (*S. coelicolor* and *M. tuberculosis*) and not with *B. subtilis* or *S. pneumoniae* DivIVAs (Fig. 4), while DivIVA$_{Bs}$ and DivIVA$_{Sp}$ interacted with each other but not with any of the actinomycete DivIVA proteins (Fig. 4).

Late localization of DivIVA at the septum. Immunolocalization studies demonstrated the frequent presence of DivIVA at the cell septum. In 20% of the 500 cells obtained from an exponentially growing culture of *C. glutamicum*, DivIVA was localized to both cell poles and to the septum; in 77%, DivIVA was detected at both poles while in only 3% of the cells the protein was found at one pole (Fig. 5A). This distribution pattern was in agreement with the localization patterns obtained when DivIVA$_{Cg}$ was fused to the reporter protein EGFP2 (DivIVA$_{Cg}$-EGFP2) (Fig. 5B), indicating that the hybrid protein behaved like DivIVA$_{Cg}$.

DivIVA recruitment to the division site at mid-cell was examined in relation to nucleoid segregation and septal PG synthesis. Visualization of PG assembly using Van-650/665 (red fluorescence) staining showed that approximately 35% of the cells stained at mid-cell lacked detectable DivIVA-EGFP2 signal at that site (Fig. 5B, horizontal arrows). In contrast, all cells with DivIVA-EGFP2 at the putative division site were stained

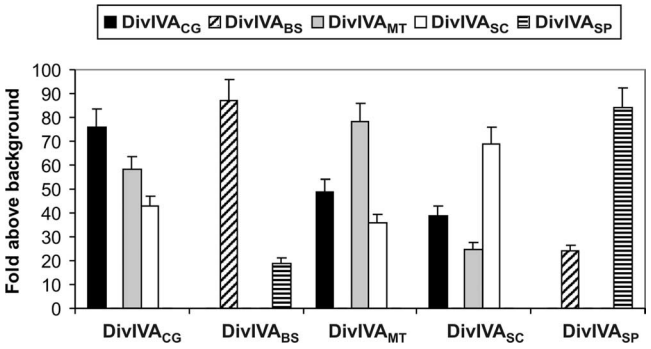

FIG. 4. Interactions between different DivIVA proteins from gram-positive bacteria analyzed in a bacterial two-hybrid system. All combinations between bait (abscises) and prey (legends) are shown. The basal growth detected in negative controls (*E. coli* BacterioMatch II transformed with the empty plasmids) was considered as the background used to represent the data. The values are the means of four independent experiments; standard deviations are indicated on the bar top. Note that the DivIVA proteins from actinomycetes interact with each other, but they do not interact with DivIVAs from *B. subtilis* or *S. pneumoniae*.

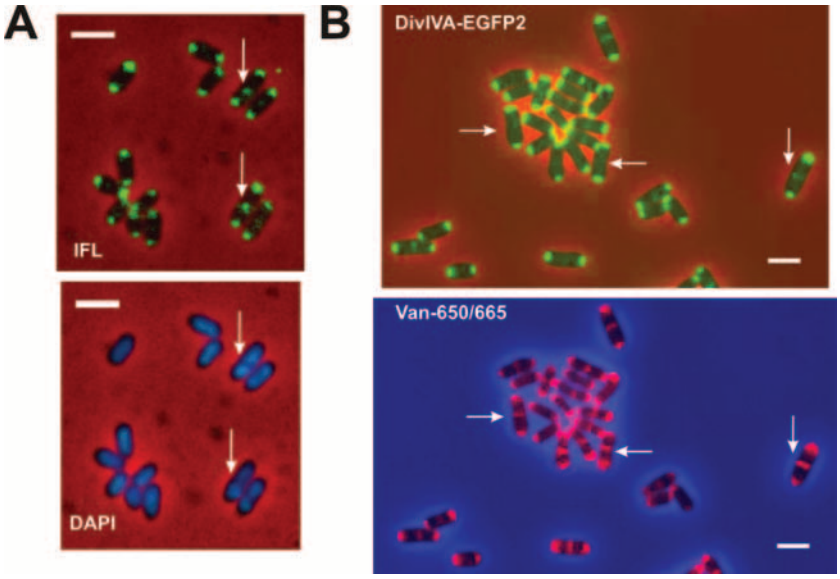

FIG. 5. DivIVA arrives at mid-cell at a late stage of cell division in *C. glutamicum*. (A) Immunofluorescence (IFL) microscopy using anti-DivIVA antiserum and DAPI staining of nucleoids in *C. glutamicum* R31. Arrows show that DivIVA localizes at the septum in cells with visibly segregated nucleoids. Size bar, 1 μm. (B) Fluorescence microscopy (EGFP2) and Van-650/665 staining of *C. glutamicum* R33, carrying an extra chromosomal copy of *divIVA*$_{Cg}$*-egfp2* under the control of P*div* (P*div-divIVA*$_{Cg}$*-egfp2*). Arrows indicate the cells in which the biosynthesis of new PG (visualized by Van-650/660 staining) has preceded septal localization of DivIVA-EGFP2 (EGFP2 fluorescence). Size bar, 1 μm.

with Van-650/665 at mid-cell (Fig. 5B, vertical arrows). Furthermore, in DAPI-stained cells containing DivIVA at mid-cell (as detected by immunofluorescence), there was always a gap between two distinct nucleoids (Fig. 5A, vertical arrows). These observations suggested that DivIVA arrives at the septum after the beginning of PG synthesis during cell division and at a stage in which the nucleoids have already visibly segregated.

DISCUSSION

Four years ago, two independent reports presented evidence supporting a role for the *divIVA* gene in the cell elongation of two different actinomycetes (19, 35). Polar localization of the DivIVA protein in *Streptomyces* and *Corynebacterium* and the striking effects on cell shape following overexpression of *divIVA* suggested that DivIVA functioned in polar cell wall synthesis. These data were confirmed very recently in another actinomycete, *M. smegmatis* (33). In that study, the authors also provided convincing evidence for the oligomerization of DivIVA$_{Ms}$ in large structures. Nevertheless, none of these three previous reports answered a fundamental question: is DivIVA essential for cell elongation in actinomycetes?

This is to our knowledge the first study showing the essential role of DivIVA in the elongation of *C. glutamicum* cells. *C. glutamicum* strains were successfully depleted of DivIVA by following two different strategies that yielded bacterial cells with similar coccoid morphologies and a lack of polar PG synthesis. These results led to the conclusion that normal levels of DivIVA are required for a rod-shaped morphology and for polarized growth by zonal PG synthesis. A similar conversion from rods to spheres is seen in *E. coli* mutants that have lost their cell-elongation systems, e.g., by depletion of MreB, MreC, or MreD or by mutation of *rodA* or *pbpA* (2, 24). Thus, it appears that *Corynebacterium*, like many other rod-shaped bacteria, has two different systems for cell-wall growth, one involving cell division and septation that can also sustain the growth of spherical cells and another for cell-wall elongation (40, 44).

Since we previously showed that *divIVA*$_{Cg}$ was essential in *C. glutamicum* and that the gene could not be deleted (35), it was surprising that the depletion of DivIVA$_{Cg}$ did not prevent growth or strongly limited viability, despite a marked loss of apical cell wall elongation. This finding suggests that the residual level of DivIVA$_{Cg}$ detected in the depletion experiments may have been sufficient to fulfill another, as-yet-unknown, essential function in *C. glutamicum*, even though participation of DivIVA$_{Cg}$ in cell wall elongation had been abolished. DivIVA arrives at the septum after cell division-related PG synthesis has already started and at a stage in which the nucleoids are already visibly segregated (Fig. 5). This late arrival of DivIVA at the division site seems to rule out a direct involvement of the protein in cell division and chromosome segregation. In addition, *C. glutamicum* cells partially depleted of DivIVA do not form chains of cells attached at the poles, as seen for streptococci (17), making it improbable that the protein is necessary for a final stage of cell division or cell-pole maturation.

The activities and polar localization of DivIVA homologues from the actinobacteria *S. coelicolor* and *M. tuberculosis* were similar to what was observed in *C. glutamicum*. However, the proteins from *B. subtilis* and *S. pneumoniae* accumulated at septation sites and interfered with growth and cell division. This revealed a functional distinction between the DivIVA orthologues of *Actinobacteria* and *Firmicutes*, in which only those of the former may be involved in zonal cell wall assembly

at the cell poles. This conclusion is consistent with the fact that neither *B. subtilis* nor *S. pneumoniae* grows in the polarized fashion typical of many *Actinobacteria* (11, 18). Interestingly, overexpression of $DivIVA_{Sc}$ in *C. glutamicum* did not lead to branching, as it does in *S. coelicolor* (19). Thus, other components needed for triggering true branching in *S. coelicolor* are perhaps absent from *Corynebacterium*.

Since $DivIVA_{Bs}$ was previously found to localize promiscuously at the cell poles of *E. coli* or *Schizosaccharomyces pombe* (16), the finding that it was not located at the cell poles of *C. glutamicum* was unexpected. One potential explanation for this result is that oligomerization of heterologous DivIVA with $DivIVA_{Cg}$ may be needed for targeting to the poles of *C. glutamicum*. Alternatively, the low levels of $DivIVA_{Cg}$ in *C. glutamicum* GNTD could have been sufficient to compete with $DivIVA_{Bs}$ and exclude it from the poles. It may also be the case that heterologous DivIVAs do not fold properly in *C. glutamicum*.

During synthesis of the bacterial cell wall, some form of internal support is required. In most rod-shaped bacteria, the Z-ring (during cell division) and the MreB helicoidal structures (during cell wall elongation) comprise a cytoskeleton that sustains PG synthesis (41). DivIVA is essential for polar growth in *C. glutamicum*, and the cellular localization of DivIVA in all *Actinobacteria* tested coincides exactly with the sites of PG synthesis during cell growth (Fig. 5B) (19, 33). Therefore, DivIVA oligomers may serve as the cytoskeletal framework for polar PG synthesis in these bacteria. In *C. glutamicum*, the late localization of DivIVA to the division septum suggests that this protein recognizes the nascent cell poles rather than an early component of the septal machinery (Fig. 5); this is consistent with the idea that DivIVA promotes the switch from septal to polar PG synthesis. Supporting this hypothesis, overexpression of DivIVA stimulates localized cell wall synthesis and increases the diameter of cell poles in *C. glutamicum* (Fig. 1B), *S. coelicolor* (19), and *M. tuberculosis* (33), implying that DivIVA is able to recruit some proteins for PG synthesis at the cell pole. We propose that when DivIVA is limiting in the *C. glutamicum* cell, it cannot efficiently form oligomers and thus cannot efficiently recruit the PG synthesis machinery. This forces the septal machinery to drive most of the PG synthesis, resulting in septal vancomycin staining and coccoid cells. When DivIVA is deleted completely, the septal machinery is forced to drive all PG synthesis but cannot support sufficient PG synthesis for cell viability. One possibility is that increased levels of FtsZ may help to drive increased septal PG synthesis under these conditions, as has been shown for spherical mutants of *E. coli* (3).

Although the above speculation suggests an interplay between FtsZ and DivIVA in *C. glutamicum*, DivIVA does not seems to be required for proper localization of the Z-ring in this species, in contrast to *B. subtilis* (9, 15). Since *C. glutamicum* lacks a MinCD system or any other known positive and negative regulators of bacterial cell division (i.e., *ezrA*, *ftsA*, *min*, *noc*, *slmA*, *sulA*, *zipA*, or *zapA*) (27) and does not undergo nucleoid occlusion (36), how *C. glutamicum* is nonetheless able to divide almost symmetrically remains unknown. Additional studies will be needed to better understand this and other aspects of cell division and cell growth in rod-shaped *C. glutamicum*.

ACKNOWLEDGMENTS

M. Letek and E. Ordóñez were beneficiaries of fellowships from the Ministerio de Educación y Ciencia and the Junta de Castilla y León, respectively. This work was funded by grants from the Junta de Castilla y León (reference LE040A07), University of León (ULE 2001-08B), and Ministerio de Ciencia y Tecnología (BIO2002-03223 and BIO2005-02723).

We thank Carlos Martín (Universidad de Zaragoza, Spain), Jeff Errington (University of Newcastle, United Kingdom), David A. Hopwood (John Innes Institute, Norwich, United Kingdom), and Orietta Massidda (University of Cagliari, Italy) for the chromosomal DNAs from the wild-type strains *M. tuberculosis* H37Rv, *B. subtilis* subsp. *subtilis* strain 168, *S. coelicolor* A3(2), and *S. pneumoniae* R6, respectively.

REFERENCES

1. **Adham, S. A., A. B. Campelo, A. Ramos, and J. A. Gil.** 2001. Construction of a xylanase-producing strain of *Brevibacterium lactofermentum* by stable integration of an engineered *xysA* gene from *Streptomyces halstedii* JM8. Appl. Environ. Microbiol. **67:**5425–5430.
2. **Begg, K. J., B. G. Spratt, and W. D. Donachie.** 1986. Interaction between membrane proteins PBP3 and RodA is required for normal cell shape and division in *Escherichia coli*. J. Bacteriol. **167:**1004–1008.
3. **Bendezu, F. O., and P. A. de Boer.** 2008. Conditional lethality, division defects, membrane involution and endocytosis in *mre* and *mrd* shape mutants of *Escherichia coli*. J. Bacteriol. **190:**1792–1811.
4. **Bierman, M., R. Logan, K. O'Brien, E. T. Seno, R. N. Rao, and B. E. Schoner.** 1992. Plasmid cloning vectors for the conjugal transfer of DNA from *Escherichia coli* to *Streptomyces* spp. Gene **116:**43–49.
5. **Bradford, M. M.** 1976. A rapid and sensitive method for the quantitation of microgram quantities of protein using the principles of protein-dye binding. Anal. Biochem. **72:**248–254.
6. **Cabeen, M. T., and C. Jacobs-Wagner.** 2005. Bacterial cell shape. Nat. Rev. Microbiol. **3:**601–610.
7. **Carballido-Lopez, R.** 2006. The bacterial actin-like cytoskeleton. Microbiol. Mol. Biol. Rev. **70:**888–909.
8. **Cerdeno-Tarraga, A. M., A. Efstratiou, L. G. Dover, M. T. Holden, M. Pallen, S. D. Bentley, G. S. Besra, C. Churcher, K. D. James, Z. A. De, T. Chillingworth, A. Cronin, L. Dowd, T. Feltwell, N. Hamlin, S. Holroyd, K. Jagels, S. Moule, M. A. Quail, E. Rabbinowitsch, K. M. Rutherford, N. R. Thomson, L. Unwin, S. Whitehead, B. G. Barrell, and J. Parkhill.** 2003. The complete genome sequence and analysis of *Corynebacterium diphtheriae* NCTC13129. Nucleic Acids Res. **31:**6516–6523.
9. **Cha, J. H., and G. C. Stewart.** 1997. The *divIVA* minicell locus of *Bacillus subtilis*. J. Bacteriol. **179:**1671–1683.
10. **Chauhan, A., H. Lofton, E. Maloney, J. Moore, M. Fol, M. V. Madiraju, and M. Rajagopalan.** 2006. Interference of *Mycobacterium tuberculosis* cell division by Rv2719c, a cell wall hydrolase. Mol. Microbiol. **62:**132–147.
11. **Daniel, R. A., and J. Errington.** 2003. Control of cell morphogenesis in bacteria: two distinct ways to make a rod-shaped cell. Cell **113:**767–776.
12. **Daniel, R. A., E. J. Harry, and J. Errington.** 2000. Role of penicillin-binding protein PBP 2B in assembly and functioning of the division machinery of *Bacillus subtilis*. Mol. Microbiol. **35:**299–311.
13. **de Pedro, M. A., J. C. Quintela, J. V. Holtje, and H. Schwarz.** 1997. Murein segregation in *Escherichia coli*. J. Bacteriol. **179:**2823–2834.
14. **Divakaruni, A. V., R. R. Loo, Y. Xie, J. A. Loo, and J. W. Gober.** 2005. The cell-shape protein MreC interacts with extracytoplasmic proteins including cell wall assembly complexes in *Caulobacter crescentus*. Proc. Natl. Acad. Sci. USA **102:**18602–18607.
15. **Edwards, D. H., and J. Errington.** 1997. The *Bacillus subtilis* DivIVA protein targets to the division septum and controls the site specificity of cell division. Mol. Microbiol. **24:**905–915.
16. **Edwards, D. H., H. B. Thomaides, and J. Errington.** 2000. Promiscuous targeting of *Bacillus subtilis* cell division protein DivIVA to division sites in *Escherichia coli* and fission yeast. EMBO J. **19:**2719–2727.
17. **Fadda, D., A. Santona, V. D'Ulisse, P. Ghelardini, M. G. Ennas, M. B. Whalen, and O. Massidda.** 2007. *Streptococcus pneumoniae* DivIVA: localization and interactions in a MinCD free context. J. Bacteriol. **189:**1288–1298.
18. **Flardh, K.** 2003. Growth polarity and cell division in *Streptomyces*. Curr. Opin. Microbiol. **6:**564–571.
19. **Flardh, K.** 2003. Essential role of DivIVA in polar growth and morphogenesis in *Streptomyces coelicolor* A3(2). Mol. Microbiol. **49:**1523–1536.
20. **Hanahan, D.** 1983. Studies on transformation of *Escherichia coli* with plasmids. J. Mol. Biol. **166:**557–580.
21. **Jager, W., A. Schafer, A. Puhler, G. Labes, and W. Wohlleben.** 1992. Expression of the *Bacillus subtilis sacB* gene leads to sucrose sensitivity in the gram-positive bacterium *Corynebacterium glutamicum* but not in *Streptomyces lividans*. J. Bacteriol. **174:**5462–5465.

22. **Kalinowski, J., B. Bathe, D. Bartels, N. Bischoff, M. Bott, A. Burkovski, N. Dusch, L. Eggeling, B. J. Eikmanns, L. Gaigalat, A. Goesmann, M. Hartmann, K. Huthmacher, R. Kramer, B. Linke, A. C. McHardy, F. Meyer, B. Mockel, W. Pfefferle, A. Puhler, D. A. Rey, C. Ruckert, O. Rupp, H. Sahm, V. F. Wendisch, I. Wiegrabe, and A. Tauch.** 2003. The complete *Corynebacterium glutamicum* ATCC 13032 genome sequence and its impact on the production of L-aspartate-derived amino acids and vitamins. J. Biotechnol. **104:**5–25.
23. **Kang, C. M., D. W. Abbott, S. T. Park, C. C. Dascher, L. C. Cantley, and R. N. Husson.** 2005. The *Mycobacterium tuberculosis* serine/threonine kinases PknA and PknB: substrate identification and regulation of cell shape. Genes Dev. **19:**1692–1704.
24. **Kruse, T., J. Bork-Jensen, and K. Gerdes.** 2005. The morphogenetic MreBCD proteins of *Escherichia coli* form an essential membrane-bound complex. Mol. Microbiol. **55:**78–89.
25. **Laemmli, U. K.** 1970. Cleavage of structural proteins during the assembly of the head of bacteriophage T4. Nature **227:**680–685.
26. **Leaver, M., and J. Errington.** 2005. Roles for MreC and MreD proteins in helical growth of the cylindrical cell wall in *Bacillus subtilis*. Mol. Microbiol. **57:**1196–1209.
27. **Letek, M., E. Ordonez, M. Fiuza, M. P. Honrubia-Marcos, J. Vaquera, J. A. Gil, and L. M. Mateos.** 2007. Characterization of the promoter region of *ftsZ* from *Corynebacterium glutamicum* and controlled overexpression of FtsZ. Int. Microbiol. **10:**271–282.
28. **Letek, M., N. Valbuena, A. Ramos, E. Ordonez, J. A. Gil, and L. M. Mateos.** 2006. Characterization and use of catabolite-repressed promoters from gluconate genes in *Corynebacterium glutamicum*. J. Bacteriol. **188:**409–423.
29. **Mateos, L. M., A. Schafer, J. Kalinowski, J. F. Martin, and A. Puhler.** 1996. Integration of narrow-host-range vectors from *Escherichia coli* into the genomes of amino acid-producing corynebacteria after intergeneric conjugation. J. Bacteriol. **178:**5768–5775.
30. **Mazza, P., E. E. Noens, K. Schirner, N. Grantcharova, A. M. Mommaas, H. K. Koerten, G. Muth, K. Flardh, G. P. van Wezel, and W. Wohlleben.** 2006. MreB of *Streptomyces coelicolor* is not essential for vegetative growth but is required for the integrity of aerial hyphae and spores. Mol. Microbiol. **60:**838–852.
31. **McCormick, J. R., E. P. Su, A. Driks, and R. Losick.** 1994. Growth and viability of *Streptomyces coelicolor* mutant for the cell division gene *ftsZ*. Mol. Microbiol. **14:**243–254.
32. **Muchova, K., E. Kutejova, D. J. Scott, J. A. Brannigan, R. J. Lewis, A. J. Wilkinson, and I. Barak.** 2002. Oligomerization of the *Bacillus subtilis* division protein DivIVA. Microbiology **148:**807–813.
33. **Nguyen, L., N. Scherr, J. Gatfield, A. Walburger, J. Pieters, and C. J. Thompson.** 2007. Antigen 84, an effector of pleiomorphism in *Mycobacterium smegmatis*. J. Bacteriol. **189:**7896–7910.
34. **Nishio, Y., Y. Nakamura, Y. Kawarabayasi, Y. Usuda, E. Kimura, S. Sugimoto, K. Matsui, A. Yamagishi, H. Kikuchi, K. Ikeo, and T. Gojobori.** 2003. Comparative complete genome sequence analysis of the amino acid replacements responsible for the thermostability of *Corynebacterium efficiens*. Genome Res. **13:**1572–1579.
35. **Ramos, A., M. P. Honrubia, N. Valbuena, J. Vaquera, L. M. Mateos, and J. A. Gil.** 2003. Involvement of DivIVA in the morphology of the rod-shaped actinomycete *Brevibacterium lactofermentum*. Microbiology **149:**3531–3542.
36. **Ramos, A., M. Letek, A. B. Campelo, J. Vaquera, L. M. Mateos, and J. A. Gil.** 2005. Altered morphology produced by *ftsZ* expression in *Corynebacterium glutamicum* ATCC 13869. Microbiology **151:**2563–2572.
37. **Sanger, F., S. Nicklen, and A. R. Coulson.** 1977. DNA sequencing with chain-terminating inhibitors. Proc. Natl. Acad. Sci. USA **74:**5463–5467.
38. **Santamaria, R. I., J. A. Gil, and J. F. Martin.** 1985. High-frequency transformation of *Brevibacterium lactofermentum* protoplasts by plasmid DNA. J. Bacteriol. **162:**463–467.
39. **Schafer, A., J. Kalinowski, R. Simon, A. H. Seep-Feldhaus, and A. Puhler.** 1990. High-frequency conjugal plasmid transfer from gram-negative *Escherichia coli* to various gram-positive coryneform bacteria. J. Bacteriol. **172:**1663–1666.
40. **Scheffers, D. J., L. J. Jones, and J. Errington.** 2004. Several distinct localization patterns for penicillin-binding proteins in *Bacillus subtilis*. Mol. Microbiol. **51:**749–764.
41. **Shih, Y. L., and L. Rothfield.** 2006. The bacterial cytoskeleton. Microbiol. Mol. Biol. Rev. **70:**729–754.
42. **Stahlberg, H., E. Kutejova, K. Muchova, M. Gregorini, A. Lustig, S. A. Muller, V. Olivieri, A. Engel, A. J. Wilkinson, and I. Barak.** 2004. Oligomeric structure of the *Bacillus subtilis* cell division protein DivIVA determined by transmission electron microscopy. Mol. Microbiol. **52:**1281–1290.
43. **Tauch, A., O. Kaiser, T. Hain, A. Goesmann, B. Weisshaar, A. Albersmeier, T. Bekel, N. Bischoff, I. Brune, T. Chakraborty, J. Kalinowski, F. Meyer, O. Rupp, S. Schneiker, P. Viehoever, and A. Puhler.** 2005. Complete genome sequence and analysis of the multiresistant nosocomial pathogen *Corynebacterium jeikeium* K411, a lipid-requiring bacterium of the human skin flora. J. Bacteriol. **187:**4671–4682.
44. **Valbuena, N., M. Letek, E. Ordonez, J. A. Ayala, R. A. Daniel, J. A. Gil, and L. M. Mateos.** 2007. Characterization of HMW-PBPs from the rod-shaped actinomycete *Corynebacterium glutamicum*: peptidoglycan synthesis in cells lacking actin-like cytoskeletal structures. Mol. Microbiol. **66:**643–657.
45. **Valbuena, N., M. Letek, A. Ramos, J. Ayala, D. Nakunst, J. Kalinowski, L. M. Mateos, and J. A. Gil.** 2006. Morphological changes and proteome response of *Corynebacterium glutamicum* to a partial depletion of FtsI. Microbiology **152:**2491–2503.
46. **Wood, J. I., and K. L. Klomparens.** 1993. Characterization of agarose as an encapsulation medium for particulate specimens for transmission electron microscopy. Microsc. Res. Tech. **25:**267–275.